

A NEW CONTACT DYNAMICS MODEL TOOL FOR HARDWARE-IN-THE-LOOP DOCKING SIMULATION

M. Zebenay¹, R. Lampariello¹, T. Boge¹, and D. Choukroun²

¹Germany Aerospace Center(DLR),Wessling, Germany,
melak.zebenay@dlr.de, Roberto.Lampariello@dlr.de, Toralf.Boge@dlr.de
²Delft University of Technology,Delft, The Netherlands , d.choukroun@tudelft.nl

ABSTRACT

One of the goals of performing a hardware-in-the-loop (HIL) simulation at the European Proximity Operation simulator (EPOS 2.0) is to simulate on-orbit docking for verification and validation of the docking phase. However, this closed-loop docking simulation is influenced by the response time delay of the EPOS 2.0 controllers and by the high stiffness of the EPOS 2.0 robots. The high stiffness causes an unrealistic high impact force which puts the safety of the facility at risk and increases the position error in the docking simulator. In addition, the controller time delay destabilizes the HIL simulation by adding energy to the system. The paper presents a new contact dynamics model tool the development of which is based on a combination of a passive and active compliance and that can be used for analysis in a hybrid simulation. This method is validated experimentally using the EPOS 2.0 facility and a standard contact dynamics model. In addition, this paper presents the effect of parameters like time delay, stiffness, damping and mass on the stability of the HIL simulation, both analytically and experimentally.

Key words: HIL simulation; Spring-dashpot; stability.

1. INTRODUCTION

Autonomous docking to a free-flying object in space is a difficult and risky operation. Therefore, means to test the docking system of a servicing spacecraft, especially during the impact phase with the target spacecraft, are of great interest.

In the concept of the HIL EPOS 2.0 hybrid simulator system, the free-floating behavior of a spacecraft is determined by a mathematical model of its dynamics. Ideally, the contact dynamics should instead be represented by the real hardware contact, since this would eliminate the necessity to model the geometrical and structural properties of the impacting satellites. From this view point, the HIL simulation concept is a combination of both

mathematical-based software and physical-based hardware. The combined simulation process is intended to take advantages of both. Considerable research has been conducted on HIL simulators for simulating Rendezvous and docking (RvD) operations of space systems [1]- [4]. The concept of such a general robotics-based contact dy-

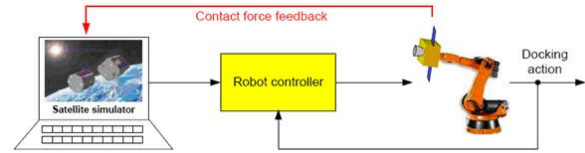


Figure 1. closed-loop HIL contact-dynamics simulator

namics test facility is illustrated by the diagram shown in Fig. 1. It consists of three basic subsystems:

- a real-time software simulator used to compute the dynamic response of the servicing and target satellites, under space environment conditions;
- two 6-DOF robots used to physically deliver the software-generated 3D dynamic motion of the satellites;
- a hardware mock-up of the docking mechanisms on the satellites, which will make physical contact operations during docking, and will measure the contact forces.

However, in order to simulate docking manoeuvres, and therefore impacts, using this concept, it is required that the robots exhibits very similar dynamics characteristics to that of the simulated satellites. Obviously, this is not possible for the industrial robots of the EPOS facility, shown in Fig. 2, because of their high stiffness. Therefore, when the robot tip is in physical contact, its compliance will differ from a free-floating satellite's one. The robot may even encounter instability in a stiff contact case. A solution is provided by adding an outer control loop onto the industrial robots (since the inner control loops cannot be modified).

An ideal approach would be to apply an impedance control strategy such as the one described in [5]. However, impedance control typically requires torque control capabilities at joint level. This is not possible for the robots of the EPOS facility. These robots have only an end-

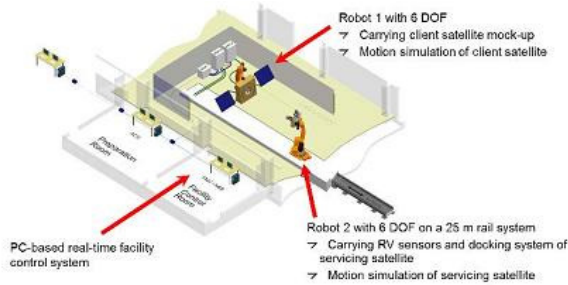


Figure 2. The new EPOS 2.0 facility: a robotics-based test bed

effector position control. Similarly, many other advanced and proven robot control strategies, such as the computed torque control [6] cannot be implemented on EPOS. Last, but not least, any active control algorithm will have problems with high frequency contacts (in the order of 1 ms) due to the robots controller intrinsic response time delay (for EPOS in the order of 32 ms).

In order to analyze the effect of the controller time delay and to reproduce the impact characteristics of the satellites a new contact dynamics model is introduced which is based on combining a mechanical compliance with a virtual compliance. The motivation of this work is to obtain any predefined stiffness and damping characteristics (within some given range), would generally require a physical replacement of the mechanical compliance for different test scenario. Instead, the method proposed here, allows to change the total compliance using software, and therefore being able to use the same mechanical compliance at the end-effector. The passive mechanical compliance is introduced between the end-effector of one robot and the docking interface probe mounted on the other robot. This is combined with an active position-based impedance controller, which can be tuned off-line to arrive at any predefined spring-dashpot contact model behavior or any other desired values. The desired predefined behavior can be dictated by a mathematical impact model for the two satellites, with known impact characteristics. The effect of the passive compliance is to lengthen the duration of the impact, thus avoiding the undesired consequences of the aforementioned time delay.

Some researchers have already proposed the use of passive compliance control for impact or contact control. Roberts [7] and Xu [8] use soft force sensors as a compliance. In [9] the use of compliance skin for the force sensor is suggested. In all these cases, the contact frequency was decreased, allowing to add an additional active control component, with the aim of improving the transient behavior of the system during transition from the non-contact to the contact phases. In recent years

several research dealt with the effect of delay and contact parameters on the stability of the system such as in haptic devices [9] [14].

The loop control is then closed by measuring the contact force between the end-effector of one robot and the docking interface probe. The measured contact force is fed back to the satellites numerical simulator, which generates the corresponding trajectories to be tracked by robots.

In this paper, the stability analysis of a HIL simulation with time delay and new contact dynamics emulation tool is presented for the 1-DOF case and validated using a spring-dashpot model on the EPOS facility. The next section briefly describes the EPOS 2.0 facility. Section 3 describes the 1-DOF docking simulation models and presents the method that determines the impedance parameters. In section 4 the stability analysis is presented. In section 5 the simulation and experimental results are presented and discussed, followed by section 6 with the conclusions.

2. EPOS 2.0-HARDWARE-IN-THE-LOOP SIMULATOR

The new EPOS 2.0 facility is aimed at providing test and verification capabilities for complete RvD processes of on-orbit servicing missions. The facility comprises a hardware-in-the-loop simulator based on two industrial robots (of which one is mounted on a 25m rail system) for physical real-time simulations of rendezvous and docking maneuvers. This test bed aims at simulating the last critical phase (separation ranging from 25 m to 0 m) of the approach process, including the contact dynamics simulation of the docking process. Fig 2 shows the main components of the facility. A detailed overview on the EPOS 2.0 facility can be found in [1].

Compared with the former EPOS facility, EPOS 2.0 has the following advances:

- It is a highly accurate test bed. The measurement and positioning performance is in submillimeter range.
- Dynamical capabilities allow for high commanding rates and allows to have the capability of force and torque measurements during contact.
- The simulations of sunlight illumination conditions as well as the compensation of Earth-gravity force are both part of the assembly to generate an utmost realistic simulation of the real rendezvous and docking process.
- The utilization of standard industrial robotics H/W allows a very high flexibility related to different application scenarios.

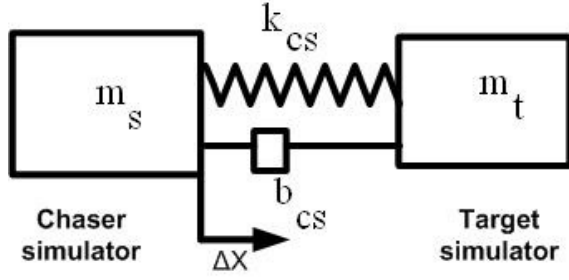


Figure 3. Ideal 1-DOF satellites impact model based on spring-dashpot contact model.

3. 1-DOF DOCKING SIMULATION

In this section the mathematical models for the ideal and the hybrid simulator are briefly presented. A method for determining the impedance parameters of the hybrid simulator is summarized based on the desired parameters of the ideal spring-dashpot contact model.

3.1. 1-DOF ideal impact model

Fig 3 shows a 1-DOF model of two satellites coming into contact, where the contact force is modeled using a linear spring-dashpot method [11].

The relative dynamics can be modeled as follows

$$\delta\ddot{x} = -\left(\frac{m_s + m_t}{m_s m_t}\right)(k_{cs}\delta x + b_{cs}\delta\dot{x}) \quad (1)$$

where δx stands for the relative position between the two satellites during contact, k_{cs} is a spring constant and b_{cs} is a velocity damping constant, m_s and m_t stand for the chaser and target satellite mass, respectively.

The equation of motion of the servicer satellite during the contact phase is simply: Double integrating (1) gives a relative position command, which can be send to the robot controllers. The robots display the motion in real time, based on the position command.

The model described in Eq.1 will serve as a reference desired behavior for determining the hybrid model, described in the next section.

3.2. 1-DOF hybrid impact model

One of the challenges of the docking simulation is to reproduce the impedance properties for a specific satellites docking case with the ground facility. A hybrid impact model is proposed in order to determine the required end-effector or Cartesian impedance of the ground facility robots, based on the mathematical model of the satellite impact dynamics.

A hybrid simulator is described here, which behaves with predefined stiffness and damping characteristics. We achieve this feature by first aiming at obtaining the same contact force, the same impact duration and the same final position and velocity, as those described by the ideal model (shown in Fig. 3). To do so, contacts are assumed to be sufficiently long, such that the robot controller time delay does not play an important role.

Fig. 4 shows the closed-loop HIL simulation setup, where the stiffness k refers to that of the mechanical compliance that is introduced at the robot end-effector, and k_1, b_1, k_2 and b_2 are the active impedance parameters to be determined, as described below, such that the total resulting impedance is the same as that of the ideal system. From Fig. 4, the equation of motion of the chaser follows as:

$$m_1\ddot{x}_1 = -k_1(x_1 - \int V_{CoM} dt) - b_1(\dot{x}_1 - V_{CoM}) - k(x_1 - x_2), \quad (2)$$

and that of the target as:

$$m_2\ddot{x}_2 = -k_2(\int V_{CoM} dt - x_2) - b_2(\dot{x}_2 - V_{CoM}) - k(x_2 - x_1). \quad (3)$$

The virtual impedances shown in the figure are attached to a virtual wall that moves with the velocity of the center of mass of the system, V_{CoM} , defined as:

$$V_{CoM} = \frac{m_1\dot{x}_1(0) + m_2\dot{x}_2(0)}{m_1 + m_2}. \quad (4)$$

The virtual wall is introduced to treat the most general case, for which the center of mass of the system is not stationary. Assuming no external forces, a frame attached to the center of mass of the system is inertial.

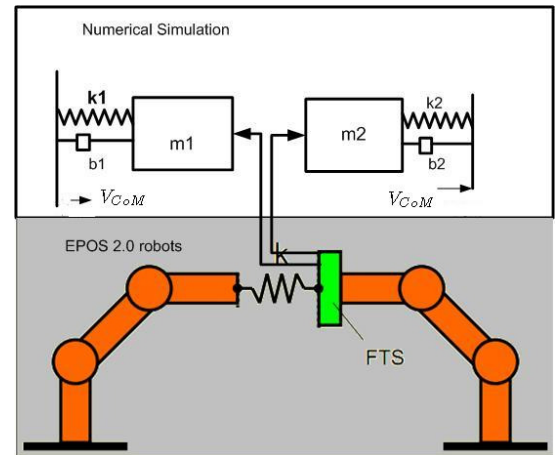


Figure 4. Closed-loop HIL docking simulation based on passive and virtual (active) compliance. The force/torque sensor (FTS) data is added to the virtual compliance data, the net force is fed back to the satellite simulator.

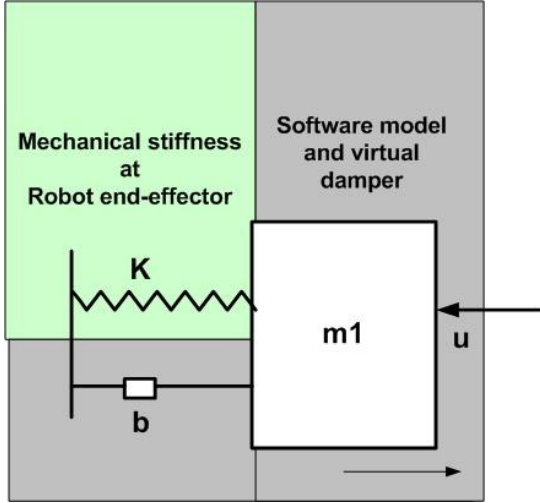


Figure 5. Simplified HIL contact model of the relative motion

The equations above can therefore be written in this frame, without loss of generality. The positions of the two satellites are then relative to the constant center of mass motion and do not involve, as such, constantly growing terms in time.

3.3. Impedance control parameter determination

An impedance behavior which is equivalent to that of the ideal satellites, results in the same dynamic response, such as the same contact force, final velocity, final position and contact duration. The determination equations of the unknowns $k_1, b_1, k_2,$ and b_2 are derived for given satellite masses m_1 and m_2 , given contact parameters k_{cs} and b_{cs} and also given stiffness k of the force sensor. In addition, the impedance model masses are given the same value as the corresponding ideal satellite masses. Hence the unknowns can be determined using the equations below, by equating the states of the ideal satellites to those of the impedance model, at two different times t_1 and t_2 see equations below. These times are chosen in the range of the contact duration which has a duration of half cycle of a force profile. Thus, the analytical solution for k_1 and b_1 can be computed as:

$$\begin{bmatrix} k_1 \\ b_1 \end{bmatrix} = \begin{bmatrix} -x_1(t_1) + V_{CoM}t_1 & -\dot{x}_1(t_1) + V_{CoM} \\ -x_1(t_2) + V_{CoM}t_2 & -\dot{x}_1(t_2) + V_{CoM} \end{bmatrix}^{-1} \times \begin{bmatrix} m_1\ddot{x}_1(t_1) - b_{cs}(\dot{x}_2(t_1) - \dot{x}_1(t_1)) - k_{cs}(x_2(t_1) - x_1(t_1)) \\ m_1\ddot{x}_1(t_2) - b_{cs}(\dot{x}_2(t_2) - \dot{x}_1(t_2)) - k_{cs}(x_2(t_2) - x_1(t_2)) \end{bmatrix} \quad (5)$$

where the states of $x_1(t)$ and $\dot{x}_1(t)$ are taken from the ideal simulation.

Similarly k_2 and b_2 can be determined as:

$$\begin{bmatrix} k_2 \\ b_2 \end{bmatrix} = \begin{bmatrix} -x_2(t_1) + V_{CoM}t_1 & -\dot{x}_2(t_1) - V_{CoM} \\ -x_2(t_2) + V_{CoM}t_2 & -\dot{x}_2(t_2) - V_{CoM} \end{bmatrix}^{-1} \times \begin{bmatrix} m_2\ddot{x}_2(t_1) + b_{cs}(\dot{x}_2(t_1) - \dot{x}_1(t_1)) + k_c(x_2(t_1) - x_1(t_1)) \\ m_2\ddot{x}_2(t_2) + b_{cs}(\dot{x}_2(t_2) - \dot{x}_1(t_2)) + k_c(x_2(t_2) - x_1(t_2)) \end{bmatrix} \quad (6)$$

The unknown impedance parameters result to be independent of the initial velocities of the two satellites. This allows to perform the determination only once, and then perform different experiments for any initial velocities.

4. STABILITY ANALYSIS WITH DELAY IN THE LOOP

The relative motion Eq.1 of the ideal one DOF satellites impact model shown in Fig. 3 can be modeled as a mass-spring damper equation which contain both the hardware contact part and the software model of the free-floating masses. The free-floating masses is reduced to a mass called reduced mass as shown in Eq.8. Fig.5 shows the modified model using the relative motion equation for stability analysis. The modified model is represented by the closed loop system as shown in Fig.6 where the transfer function of each block are described as follows.

$$\begin{aligned} H_1(s) &= \frac{X_r(s)}{F_{in}(s)} = \frac{1}{m_1 s^2} \\ H_2(s) &= \frac{X_c(s)}{X_r(s)} = e^{-sh} \\ H_3(s) &= \frac{X_m(s)}{X_c(s)} = e^{-sh} \\ H_4(s) &= \frac{F(s)}{X_c(s)} = -K - bs \\ H_5(s) &= \frac{F_m(s)}{F(s)} = 1 \end{aligned} \quad (7)$$

where

$$m_1 = \frac{m_s m_t}{m_s + m_t} \quad (8)$$

where

$X_r(s)$ is the required position command from the free-floating model.

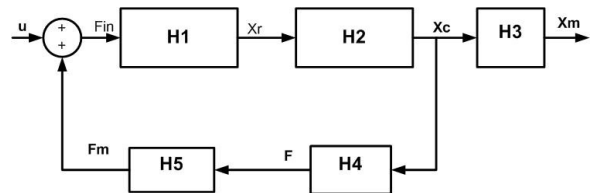


Figure 6. Simplified block diagram of the HIL simulator

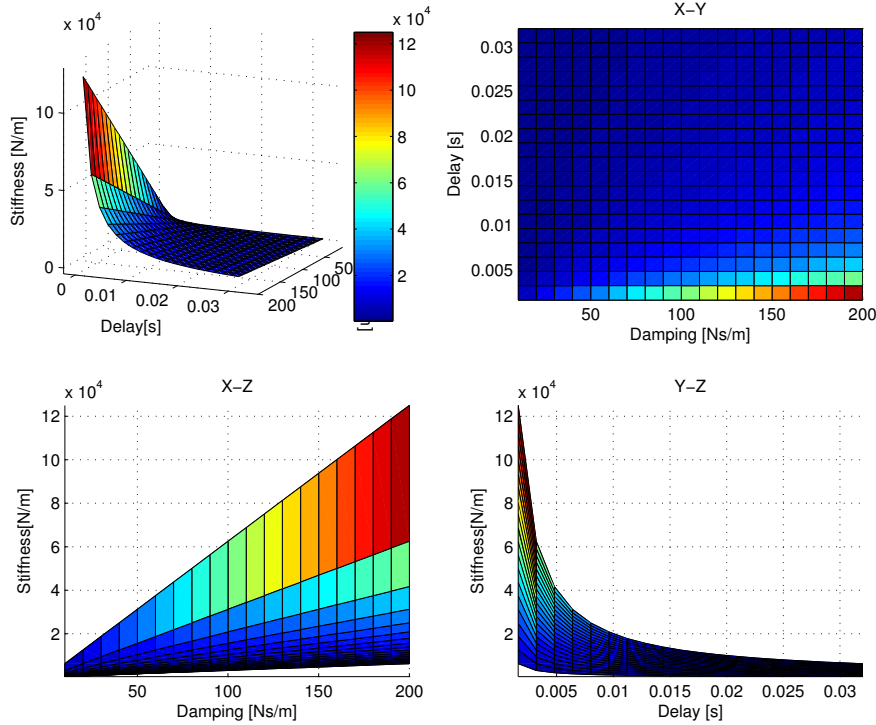


Figure 7. Critically stable plane for $m_1=750\text{kg}$, $10 < b < 200\text{Ns/m}$ and $16 < h < 32\text{ms}$

$X_c(s)$ is the current relative position of the robot end-effector.

$X_m(s)$ is the measured relative position of the end-effector.

$F_m(s)$ is the measured contact force.

$F(s)$ is the real force.

K is the contact model stiffness.

b is the contact model damping property

h is the time delay of the robot controller,

m_1 is the reduced free-floating point mass.

The transfer function of the closed-loop system from the position output X_m to the input force U is written as:

$$H(s) = \frac{X_m(s)}{U(s)} = \frac{\frac{1}{m_1 s^2} e^{-s2h}}{1 + e^{-sh} \frac{K+bs}{m_1 s^2}} \quad (9)$$

In order to analyze the stability of the system using classical method in a closed-loop system as a function of stiffness, damping and time delay of the controller the transfer function has to be written as rational function. However delay element is infinite-dimensional(irrational function),which complicates its treatment. Thus the delay element needs to be approximated using finite-dimensional(rational) elements. Some of the methods that can be used to approximate the transfer function of time delay are Taylor, Bessel-Thomson and Pade approximation. Among these methods the Pade approximations is the most widely used. [12], [13]. The first order Pade

approximation is expressed as Eq.10:

$$e^{-sh} = \frac{2 - sh}{2 + sh} \quad (10)$$

Using Eq.10 the closed-loop characteristic equation is rewritten as follows Eq.11.

$$1 + \frac{K(2 - hs)}{m_1 h s^3 + s^2(2m_1 - hb) + 2bs} = 0 \quad (11)$$

The Routh's stability criteria is used in order to determine the stability regions for different values of m_1 , K , b and h . This method yields the range of gain for which the closed-loop system is stable. Assuming the known positive values of h , m_1 and b to have stable system or all roots to be the left half plane the values of K should be in the following range.

$$0 < K < \frac{b(4m_1 - 2bh)}{h(4m_1 - bh)} \quad (12)$$

Fig.7 shows the 3D plot and 2D projections of the critically stable plane using Eq.12. The 3D plot shows that the stable region is bounded in the stiffness axis from the plane shown and zero stiffness ,

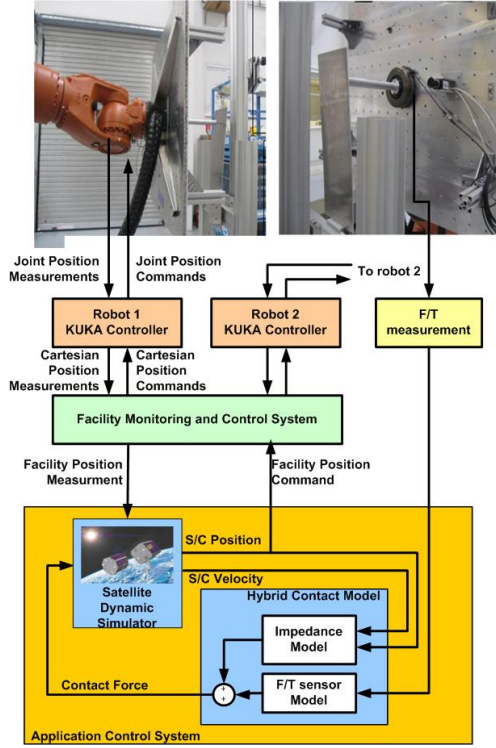


Figure 8. Validation of the new contact model tool using EPOS 2.0 robot as a chaser and a target metal sheet ($k \approx 1000N/m$) attached to a fixed structure

from the damping axis $10 < b < 200Ns/m$, from the time delay axis from $0.0016 < h < 0.032ms$ for a free-floating mass of 750kg. Note that in order to be closer to natural contact (without time delay) the damping added to stabilize the system should be kept as small as possible and the maximum stiffness is limited by the bandwidth of the EPOS 2.0 controller and the desired contact force error accuracy compared to the contact force without time delay.

5. RESULTS

Both simulation and hardware experiments were performed to validate the equivalence of the ideal spring-dashpot and the hybrid contact dynamics models. Figs. 4 and 8 show the simulation and the hardware setups, respectively.

For the hardware setup, only one robot was used, to impact against a metal sheet with a passive compliance. This was done for safety reasons. As a result, the impact durations were also relatively long. The force/torque sensor measurements of the contact force, were added to the impedance controller output (which computes the virtual forces based on the determined contact parameters and on the relative states of the satellites simulation) and fed back to the satellite dynamics numerical simulation. The latter provided the motion states which were send as po-

Table 1. Ideal and computed hybrid model parameters.

Parameters	Ideal Model	Hybrid Model
$m_1 [kg]$	750	750
$m_2 [kg]$	10^6	10^6
$k_{cs} [N/m]$	3000	-
$b_{cs} [Ns/m]$	40	-
$k_1 [N/m]$	-	2001.5
$b_1 [Ns/m]$	-	40.03
$k_2 [N/m]$	-	2668700
$b_2 [Ns/m]$	-	53373
$\dot{x}_1(0) [m/s]$	0.03	0.03
$\dot{x}_2(0) [m/s]$	0.0	0.0

sition commands to the robots.

For the known contact parameters k_{cs} and b_{cs} of the ideal model, and their corresponding masses m_1 and m_2 , and for a known fixed passive compliance k , the equivalent impedance model parameters k_1 , b_1 , k_2 , b_2 were determined.

5.1. Verification of the new contact model tool

The active impedance model parameters were determined using Eqs.5-6. The values of the ideal satellite simulator and the computed hybrid satellites model is summarized in Tab. 1. The hardware stiffness was measured to be $k=1000N/m$, at the specific position of the impact on the metal sheet, which was attached to a fixed structure and simulated the target of mass m_2 .

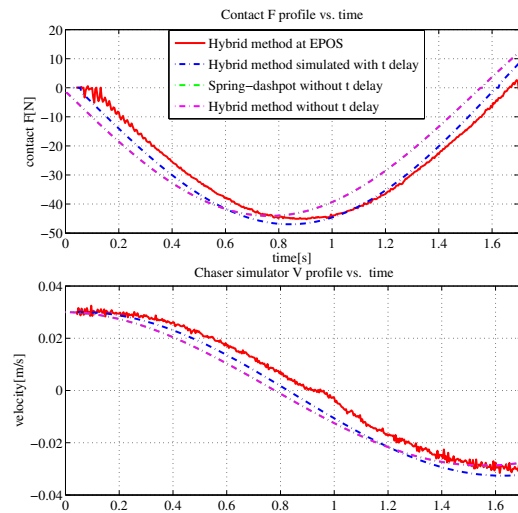


Figure 9. Contact force and velocity profile of hybrid model validation using Spring-dashpot method

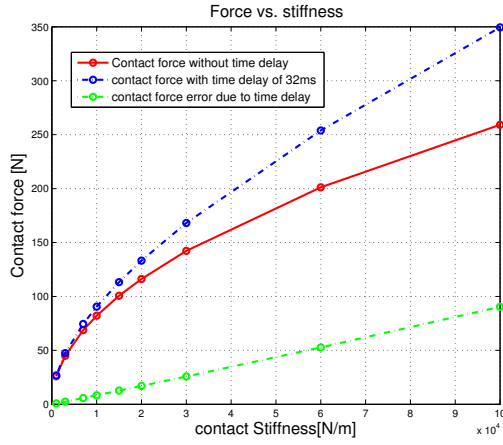


Figure 10. Contact force vs. stiffness relation with and without time delay of 32ms

Comparing to m_1 , m_2 is chosen very big to simplify the experiment using only one robot and a fixed structure which will simulate the same initial and final velocity due to the high inertia. Fig. 9, the first two cases, shown with a rose and green dotted line, are comparing the simulation result for the ideal model and the hybrid model (without time delay).

The third case, shown with a blue dotted line, is the numerical simulation of the HIL with a time delay of 32ms. The fourth case, shown with a solid red line, is the experimental result using the EPOS facility.

The velocity profiles for the first two cases are identical which can be seen on the overlap of the green and rose color. However, for case three and four the results are not exactly the same.

This may be attributed to a possible estimation error for the stiffness k , time delay, unestimated natural damping of the metal sheet and the sensor noise.

Fig. 9 also shows the comparison between the simulated and measured contact force profiles, applied at the center of mass of the chaser satellite. Comparing the peak value of the force shows an error of around 1.0N. This can be attributed to the force/torque sensor accuracy and to the robot controller time delay which causes adding energy to the system. Furthermore, this error increases as the stiffness of the mechanical compliance increases. Fig. 10 shows simulation result of the relation between the contact force and the contact stiffness with and without delay.

5.2. Verification of stability analysis using EPOS 2.0

In order to validate the stability region experiment is performed using similar to Fig. 8 setup at EPOS 2.0 facility. In this setup a constant thrust force of 10N is applied to the satellite simulator for the duration of an experiment which simulate the capturing mode of the docking

phase. The corresponding trajectory is sent to the EPOS 2.0 robot controller. The robot executes the command and contacts by a probe tip a metal sheet that has a stiffness of 2510N/m which is estimated using Hooke's law. The motion has oscillatory behavior for the repeated compression and extension of the target which could be unstable or stable depend on the added virtual damper as demonstrated on Fig.11.

Based on Eq.12 of a known $m_1=750\text{kg}$, $h=0.016\text{s}$ and $b=20\text{Ns/m}$ the range of stiffness is computed as $0 < K < 1250\text{N/m}$. Similarly for the same parameters except $b=60\text{Ns/m}$ the range of stable stiffness is computed as $0 < K < 3748.8\text{N/m}$. For each experiment the damper is applied virtually using the developed contact model tool.

Fig.11 shows the expected instability results for $b=20\text{Ns/m}$ and Fig.12 shows stable result for $b=60\text{Ns/m}$.

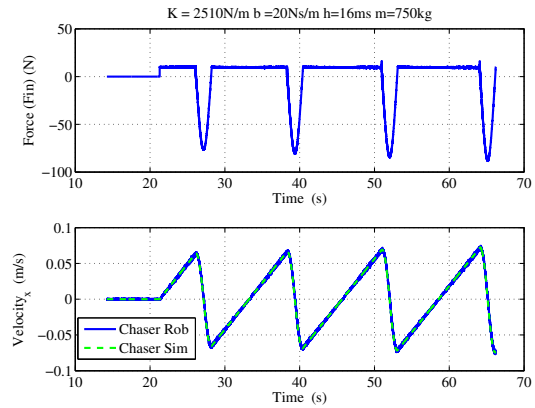


Figure 11. Expected instability for $b=20\text{Ns/m}$ using EPOS 2.0

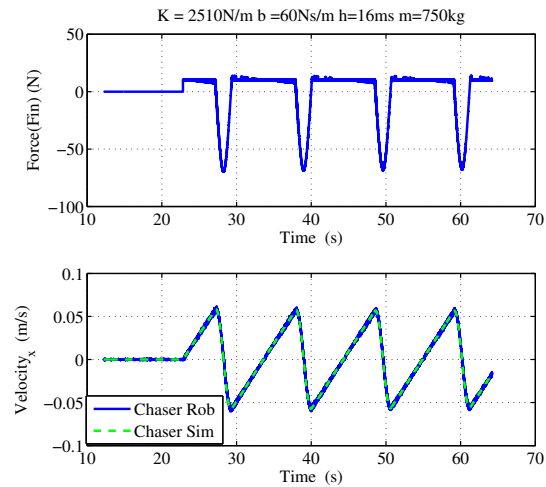


Figure 12. Expected stability for $b=60\text{Ns/m}$ using EPOS 2.0

In other words when the virtual damping is $20Ns/m$ the contact force and the corresponding velocity magnitude increases.

However when the damping is $60Ns/m$ the contact force and there corresponding velocity doesn't show increase in magnitude both for force and velocity. The result shows the 1st order Pade approximation gives reasonable result to know the stability boundary of the system which can be improved by increasing the order of approximation.

6. CONCLUSION AND FUTURE WORK

With the new presented tool for emulating impacts, it was demonstrated in simulation and in experiments that HIL impacts can be performed safely for a wide range of impact parameters. Due to the introduction of a suitably tuned active impedance control element, in conjunction with a passive compliance, changes in the impact properties to represent any system at hand, are achieved in software and not by modifications in the hardware.

The stability analysis shows that the time delay in the contact operations causes instability by adding energy to the system. The relationship between the masses of free-floating bodies, the damping, the stiffness and the time delay is derived using 1st order Pade approximation. This relationship is used to derive the EPOS 2.0 facility docking simulation stability boundary.

In the future the method will be extended to more than 1-DOF and a controller will be designed based on time-domain passivity [10].

REFERENCES

- [1] T. Boge, T.Wimmer, O.Ma, M.Zebenay, EPOS-A Robotics-Based Hardware-in-the-Loop Simulator for Simulating Satellite RvD Operations, i-SAIRAS 20010, Sapporo, Japan, August 29-September 1, 2010
- [2] F.D. Roe, R.T. Howard, and L. Murphy, Automated rendezvous and capture system development and simulation for NASA, Proc. SPIE, Vol. 5420, 118 (2004); doi:10.1117/12.542529.
- [3] O. Ma, J. Wang, S. Misra, and M. Liu., On the validation of SPDM task verification facility, Journal of Robotic Systems, Vol.21, No.5, 2004, pp. 219-235.
- [4] K. Yoshida, H. Nakanishi, H. Ueno, N. Inaba, T. Nishimaki and M. Oda, Dynamics, control and impedance matching for robotic capture of a non-cooperative satellite,Advanced Robotics 18,175198.
- [5] N. Hogan, Impedance control: An approach to manipulation, Parts I-III, ASME J. Dynam. Syst., Meas., Contr., vol. 107, pp. 1-24, 1985.5.
- [6] R.H. Middleton and G. C. Goodwin, Adaptive computed torque control for rigid link manipulations, Systems and Control Letters, Vol. 10, Issue 1, January 1988, p9-16.R.
- [7] Roberts, R. K. The Compliance of End Effector Force Sensors for Robot Manipulator Control. Ph.D.thesis, Department of Mechanical Engineering, Purdue University, 1984.
- [8] Xu, Y., and Paul, R. On position compensation and force control stability of a robot with a compliant wrist. Proceedings of the IEEE Conference on Robotics and Automation, pp. 1173-1178, 1988.
- [9] An, C.,and Hollerbach, J. Dynamic stability issues in force control of manipulators. Proceedings of the IEEE Conference on Robotics and Automation,pp. 890-896, 1987.
- [10] R. Krenn, K. Landzettel, T. Boge, M. Zebenay Passivity Control for Hybrid Simulations of Satellite Docking, ICRA11 Space Robotics Workshop May 13, 2011, Shanghai, China.
- [11] G. Gilardi, I. Sharf, Literature Survey of contact dynamics modeling, Mechanism and Machine Theory 37 Dept. of Mechanics Engineering, Victoria, Canada ,2002, 1213-1239.
- [12] M. Vajta, On Pade approximations of a dead-time, Internal Report, Dept. of Mathematical Sciences, University of Twente, 2000.
- [13] D. John, Continuous and Discrete Control Systems. Georgia Institute of Technology, 2 ed., 2002.
- [14] J.J. Gil, E.Sanchez, T.Hulin, C.preusche, and G.Hirzinger, "Stability boundary for haptic rendering: Influence of damping and delay," Journal of Computing and Information Science in Engineering,vol. 9, no.1,pp.011005-8. Mar. 2009